

# Experimental and Numerical Assessment of the Impact Test Performance Between Two UHSS Toe Cap Models

Nuno Peixinho<sup>a</sup> , Sérgio Costa<sup>b</sup>, João Mendonça<sup>a</sup>

<sup>a</sup>Universidade do Minho, Departamento de Engenharia Mecânica, Campus de Azurém, Guimarães, Portugal.

<sup>b</sup>Bairrimoldes, Anadia, Portugal.

Received: March 28, 2022; Revised: August 18, 2022; Accepted: September 04, 2022

This paper presents an integrated approach for an ultimate high-performance safety toe cap with significant milestones in slim design and weight saving. The study of crashworthiness properties was performed through impact-crash test conditions exploring the potential of applicant solutions by the combination of an advanced high-strength steel and enhanced geometric stiffening models. The structural response for a significant thickness reduction was assessed and it provides an evolved discussion for improvements in energy absorption capacity. The present case study focuses on two geometric models from the S3 slim toe cap development by prototypes made of a martensitic 1200 steel alloy. The comparison of results is complemented using numerical simulation models with mathematical description of the dynamic plasticity behaviour by applying a constitutive Cowper-Symonds equation with fundamental parameters for material strain-rate dependence.

**Keywords:** *High strength steel, numerical simulation, impact, safety toe cap.*

## 1. Introduction

The safety footwear, in the context of the global evolution of the footwear product, should adopt creative and diverse orientations. Particularly, fitting into the class of a high-performance product as a main active element in the occupational accidents prevention and Personal Protective Equipment (PPE), it is appropriate that its optimization solution amplifies the market targets, mainly combining ergonomic aspects, biological and mechanical features since its conception. The integrant toe cap component of the safety footwear is a key element by what it represents in terms of weight contribution due to the normative framework required. Hence, the continuous demand for a weight saving and the consequent comfort increase of use and issues related to occupational health have been restricted only by the highest normative commitment of this protection category. The evolution of the toe cap member with technological developments based on normative requirements and combined with a set of conditions, increasingly associated with the product as a footwear concept, fashion and versatile functionality, have boosted new trends into the safety sector. Nevertheless, the latest literature reviews have pointed out that ongoing developments remain based upon historical concepts and, therefore, for the next generation of safety footwear, a radical change is required due to the poor comfort, fit and aesthetic appeal offered by current solutions<sup>1-3</sup>.

Critical factors such as the overall weight or the required active volume of the HPF in use is still a concern with repercussions on fatigue and active potential accidents during a standard average utilization<sup>4</sup>. This is the point

where the present case study under research intended to emerge. Most of the current and reference solutions do not potentiate all the variables, in particular, the non-metallic solutions, following the trend of the recent years for weight optimization but struggling to balance the higher conceptual volume involved. In general, the relevant developments have been exploiting advanced polymeric compounds as base material solutions. The low-density structures mainly made of reinforced polyester composites with glass fibre, carbon and multi-layered nano-manufactured polymers reveal increasing potential for performance in crashworthiness behaviour and thus have been applied as the ultimate references in the safety toe cap component<sup>5-8</sup>.

The use of light-weight solutions must also be in balance with requisites of recyclability, comfort and usability. Recent works on the subject have highlighted lack of comfort of protective shoes<sup>9</sup> and a need for more women oriented designs. Life-cycle analysis presents disadvantages for polymer and composite solutions<sup>10</sup>, in contrast to their impact strength behaviour<sup>11,12</sup>. Therefore, there is an opportunity for high-strength metallic solutions to be competitive if allowing for slimmer geometries while having favourable recyclability.

The present research intended a disruptive approach in this area by developing an advanced solution that is based on a greater energy absorption capability due to the formulation of a specific geometric model, widely combined with the application of ultra-high-strength steels, which leads to a substantial weight reduction, but at the same time, it promotes dimensional space saving related to aesthetics effects of a new slim solution. That purpose follows the intensive development of other optimized technical solutions with

\*e-mail: [peixinho@dem.uminho.pt](mailto:peixinho@dem.uminho.pt)

potentiated metal alloys to manufacturing processes, across other application fields, such as the advanced aeronautics or the leading automotive industry with functional performance for impact events<sup>13,14</sup>. This work studied toe cap models with significant body-shell thickness reduction till 1.0 mm involving a high ratio of mechanical strength. The solution approach has challenged some complex phenomena's as structural stiffness, dynamic work hardening and crashworthiness properties with dynamic deformation resistance. The behavioural responses under impact test conditions were improved throughout strategical local stiffening forms and the role play of the enhanced AHSS materials was related to predictable strain rate sensitivity, which despite this range of higher characterized resistance values, can perform an accurate description in this high strength steel application context<sup>15-17</sup>. This paper brings an extended comparison of the impact testing performance between two final prototype models from the S3 slim toe cap development, and it does complement the numerical analysis with the FEA models with constitutive modelling of Cowper-Symonds equation for the UHSS martensitic 1200 steel here in evaluation and which can be assessed in depth in the reference<sup>18</sup>.

## 2. Experimental Impact Testing

The toe cap prototypes under assessment represent the final stages of development from the conception to the rehearsal for further performance testing, with higher TRL's levels by the stabilization and control of the sheet metal forming processes. Two geometric models, represented in Figure 1, were analysed by the crashworthy performance response. The S3F3 series represents the following release of the predecessor S3F2 series and aimed to exploit an improved interpretation of a new deformation path, promoted by a reformulated hardened-state lightweight body-shell, to respond more integrated with enlarged stiffening zones strategically and functionality conceived to be enhanced with a beneficial base curvature. Furthermore, prototypes of equivalent size of reference with structural thickness within 1.2 and 1.0 mm made of the same AHSS raw material of martensitic 1200M were selected.

The current study is rated under the most demanding laboratory certification of the impact resistance test – EN ISO 22568-1; 20345:2019<sup>19</sup>. When the toe caps are tested in accordance with the method described in reference<sup>19</sup>, the clearance under the toe cap for loading test conditions shall not be less than a fixed value accordingly to the toe cap size range. For the prototypes used in this study, the respective internal minimum clearance value is 21.5 mm. The test

method comprises an impact apparatus, incorporating a steel striker of mass ( $25 \pm 0.29$ ) kg, adapted to fall freely on vertical guides from a predetermined height to give the required impact energy calculated as the potential energy (drop test). The hardest parameters for the total safety level were used with a crash energy level of  $200 \pm 4$  J, promoted on the upper toe cap surface, and suitably constrained in the lower region at the time of the attack contact. In Figure 2, a deform S3F3 toe cap prototype during the normative test is represented.

The crashworthiness properties are certainly under the focus of the impact mechanics, in an implicit form, when the behaviour of structures is interrelated to dynamic solicitations. Aspects, such as the effects of inertia and the absorption of impact energy, are of most importance for the perception of this case study of application. In this context, the experimental method included a high-speed videographic system to acquire on time quantitative data during the impact events. Thus, properties for analysis, such as, displacements, linear velocities and accelerations were obtained by a Photon Ultima APX-RS camera through video sequences, for each experiment, and then processed by the image tracking software, TEMA Motion. The technical procedure, preparation, as well as other main considerations can be found in references<sup>20,21</sup>.

The toe cap prototype impact tests were used primarily to determine crushing forces – the maximum  $P_{max}$  and the mean value  $P_m$ , absorbed energy  $E_a$  and, furthermore, to assess a qualitative perform of the impact behaviour that necessarily went through the analysis of folding initiators, located deform, body side opening, and collapse modes, as patterns aligned with the loss or stiffening of structural resistance. The time course of the load striker in the drop-impact test provided enough information to obtain axial displacement-time, linear velocity-time, acceleration-time and, consequently, load-time histories for the set of experiments. It was then possible to manipulate and relate them, for instance, in function of displacement. The final crushing distance,  $\delta_f$ , was defined by the analysis of inversion of the velocity signal at the approximate interval in which the striker's velocity reaches zero and properly reviewed with the evaluation of the internal clearances in experiments, by the difference values, accurately measured prior to and after testing. Respecting this deflection interval  $\delta_f$ , the created force-displacement curve was integrated to determine the mean crushing load  $P_m$ . One of the determining factors in the study of crashworthiness is the impact energy absorption

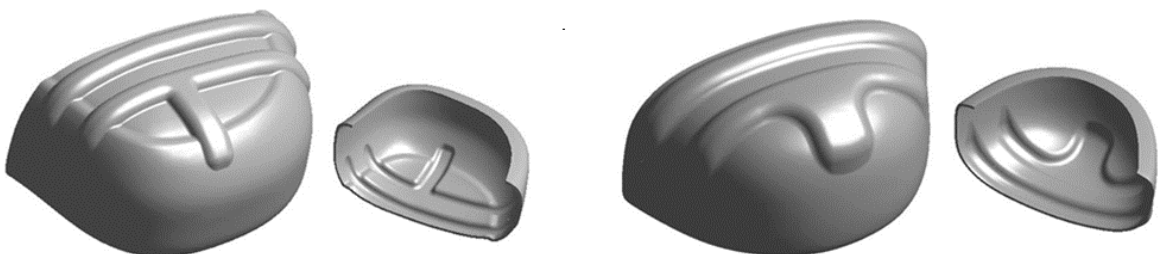


Figure 1. Conceptual S3 toe cap models.

capacity of a structure and it is linearly related to the mean crushing load by the fundamental expression<sup>15</sup>:

$$P_m = \frac{E_a}{\delta_f}$$

Therefore, by analysing the structural efficiency, the mean load parameter can be an indication of its energy-absorbing ability, when compared to the axial displacement required to absorb that energy, and due to the thickness optimization purposes it was relevant to consider the specific absorbed energy  $E_d/w$ , as an evaluation of impact performance by the unit of mass of each prototype model.

### 3. Numerical Model

The finite element analysis of the impact context was developed in order to reproduce, predict and study the experimental lab conditions observed and submitted to the toe cap prototypes. The software ANSYS Workbench from the Explicit Dynamics system with Autodyn solver was used and a simulation model set has been defined in common for both different variants made of the corresponding application of the toe cap series, which was formulated by three independent parts: the mentioned toe cap body (1:1 scale) that performs the numerical analysis, and its pair of interaction components, formed by a representative striker body – the impaction producer, and the bottom layer for the constrained support of the toe cap tab. Initial variables at the time of the contact problem, assumptions, and related considerations were properly embodied and can be found in reference<sup>19</sup>. In particular, the material modelling methodology with the integration of constitutive parameters. The summary of the numerical constitutive model selected for this discussion with the parameters collected and further modelled in simulation by the C-S equation is presented in Table 1. In Figure 3, the FEM model is represented and highlighting the generated shell mesh with triangle-based prism elements.

The toe cap model was discretized into triangle-based prism elements with sizing mesh control and the other solid parts were simplified using tetrahedral second-order structural solid elements with refinement on contact zones. The mesh sensitivity was studied to compromise run-time efficiency with desirable accuracy. Thus, a total mesh with skewness indicator of evaluation (mesh metric) of reference and an average value of 0.20 and maximum value of 0.87 was taken (Figure 3-b). The overall mesh model combines 90318 elements and 22836 nodes, distributed by the three parts. This combination results from convergence tests that are detailed in reference<sup>21</sup>.

A specific consideration is though briefly mentioned in this paper: Boundary conditions as the contact interactions - A set of different boundary conditions were applied in Workbench to perform a simulation of a dynamic loading event with the conditioning environment scene. Initial conditions were commonly defined by initial velocities and optional pre-stress states, at selected nodes or geometric parts, previously characterized, and the time variation of quantities is specified by a load curve for an end time defined. The main point in study from this topic was the set developed of different frictional interface models between the contact promoted with the lower toe cap tab region. That was crucial to be able to perform adaptive deform behaviour modes. In this paper, the discussion of results carried out two of them that figured out as improvement conditions for the simulation models. Table 2 summarizes both frictional interface models used in this case study.

### 4. Results and Discussion – S3F2 vs S3F3 series

The impact testing results are confronted to summarize on fundamental differences in the evolution of crash performance by exposed features. Equivalent proof variants within 1.0 and 1.2 mm of thickness with the same martensitic 1200M raw material were used for both series – the previous S3F2 and

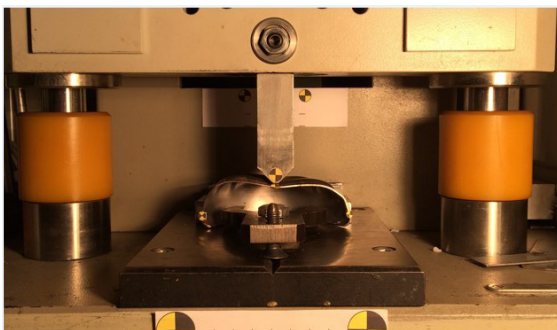


Figure 2. Normative impact test scenario focused on the striker contact.



Figure 3. Finite Element model with mesh preview of S3F3 – 1.2 mm.

Table 1. Summary of the numerical model used for Mart1200.

Numerical model ref.	Equation	Direction	Strain rate (s <sup>-1</sup> )	Constitutive Parameters	
		(°)	ref. Stress	D (s-1)	q
M12-CS6	Cowper-Symonds	90	0.00025-100   UTS	22521928.7	3.89

Parameters of the modified Hollomon equation for transverse material orientation (90°): A = 1184 (MPa); B = 828 (MPa); n = 0.36

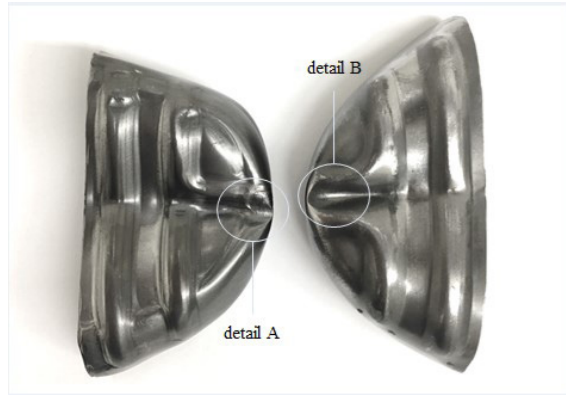
**Table 2.** Summary of the frictional interface models used in this paper.

Interface model	Summary definition
frict.1	Threshold event - full sliding effects with kinematic interaction coefficient to 0. Total unclamping conditions.
frict.2 ( $\mu 0.16$ )	Controlled sliding conditions simulated with high slippage factor allowed. Friction coefficients within 0.16 to 0.10 selected manually.

for the latest S3F3 model. The S3F3 conceptual model promotes a significant progress across the board in terms of the overall performance improvement in the context of impact resistance. Comparatively to its precedent S3F2 series, it transpires a set of relevant guidelines that were put together in a corrective behaviour analysis for the expected achievement of improvement in results. Figure 4 highlights one of the main interventions operated in the redesign process, with decisive repercussion on the potential of the obtained performance. The tendency for lateral deviations created on the top of the toe cap surface (detail A), between the impact strike contact region and the ribbed areas, intentionally idealized to receive it and specially at the frontward stiffening zone, became impossible and unpredictable to avoid in the previous series, and it contrasts with a damage line centrally positioned in the final prototype model (detail B). The results for assessment can be found in the following figures, with deformed shapes after test for both models in the Figure 5, the comparison of velocity-time histories and load-crushing displacement histories of the experimental test for different prototypes in graphs of the Figures 6 and 7, the comparison of the same results of interest with numerical results in the Figures 8 and 9. In Figures 10 and 11, numerical deformed shapes with highlighted principal stress values are comparatively illustrated. Table 3 gathers the result values of the impact test for the main properties in study.

The analysis of the geometric model contribution for the same thickness of 1.2 mm demonstrates two distinctive periods, clearly divided by the transition made by the effects in the S3F2 model described above. As can be seen in the velocity and load evolutions from the Figures 6 and 7, it shows a better initial response and then undergoes an inversion as characterized by the phenomenon of accommodation of a new concentrated impact region outside the formed rib. Consequently, it led to a turning point when juxtaposed against the corresponding S3F3 final prototype results, e.g., at approx. 6 mm of crushing displacement for load history evaluation, where its performance on the test started becoming considerably inferior until the end, even though, considering a final recover during the final stage of more intensive deformation conditions. These assumptions are also supported with the results collected in Table 3, which the energy calculation for the first 5 mm of impact deformation shows values more than the double for the first prototype series and it contrasts in the opposite order of very different final values instead.

This remark was important during the development of the final series for the interpretation of a favourable balance between all stages, in particular, carrying out the aforementioned frontal region improvement, with decisions on work definition required, plus, under a complex model of interdependence to the whole structural body. The S3F3 prototype has increased crashworthy properties under conditions of higher

**Figure 4.** Top view of the damage zone after impact – comparison of experimental prototypes.

instability, unclamped and sliding situations, which were primed by the reformulated basis framework model and in strategic drawn-out stiffeners. The results show linearity in the resistance to deformation, without interruption of the reaction in the load increase and with minor irregularities. Figure 5 illustrates local differences that relate a pattern of different deformation modes. For both deformed shapes after test, a larger damage locally caused by the load striker in the contact zone is observed for the intermediate model, with more pronounced indentation and, therefore, with further repercussion also in the same zone wherein the margin for the approval (and protection) is measured. Thus, S3F3 and the previous prototype S3F2 obtained different normative ratings, with approval and non-approval indications, respectively. As a slimmer model, The S3F3 approximates equal mass values, which potentiate even more the straight comparison of absorbed energies per weight (correctly filtered by assuming the approved interval of interest). S3F3 and S3F2 prototypes with thickness of 1.2 mm present, respectively, 3504.96 J/kg and 2170.76 J/kg.

The work role played by the S3F3 deformation mode can also be interpreted from Figures 8 and 9 through an equivalent maximum stress gradient from the simulation models at the lower dislocation position, strategically sliding the side walls to ensure continuous structural response in a stiffening reaction exercise but holding the creased deformation in the central area. Differing with lower stress values in the front end and in the indentation region than the S3F2 numerical model. The most controlled and assertively consistent deformation behaviour performed by the S3F3 series brings benefits to the numerical modelling, achieving thus a very well accuracy in the impact test results and hence leading to a worthy resource for the prototype development. The characterization of an applied friction interface model has improved the simulation analysis as well as the previous



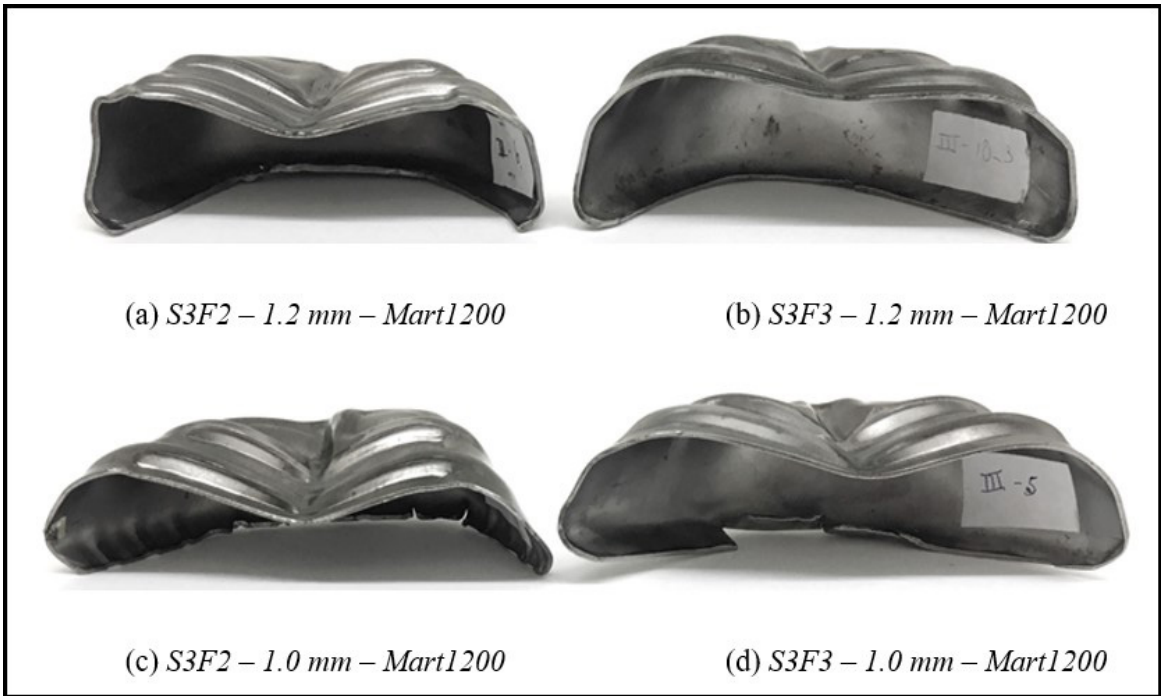


Figure 5. Experimental deformed shapes after test.

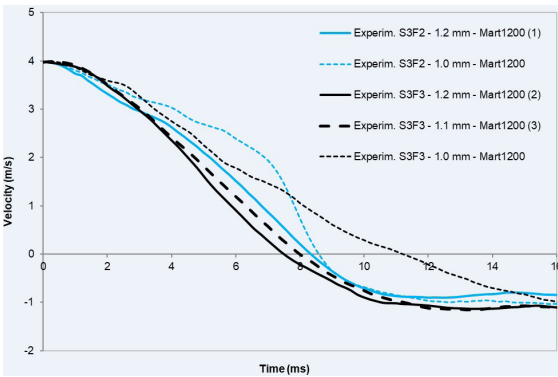


Figure 6. Comparison of velocity-time histories of the experimental test for different prototypes.

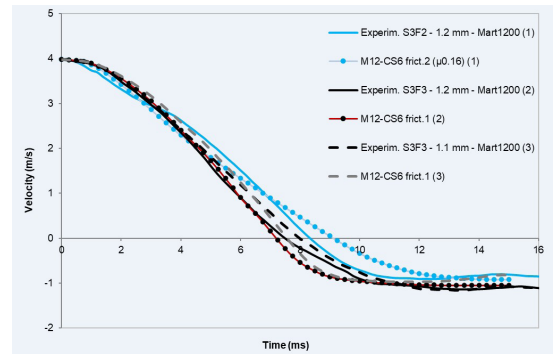


Figure 8. Comparison of velocity-time histories of the experimental test for different prototypes and respective numerical models (index in parentheses is used to correspond the respective numerical model).

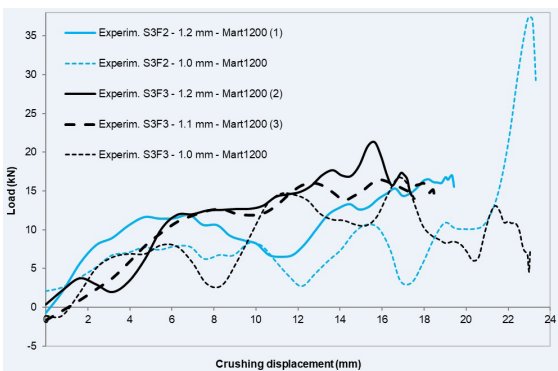


Figure 7. Comparison of load-crushing displacement histories of the experimental test for different prototypes.

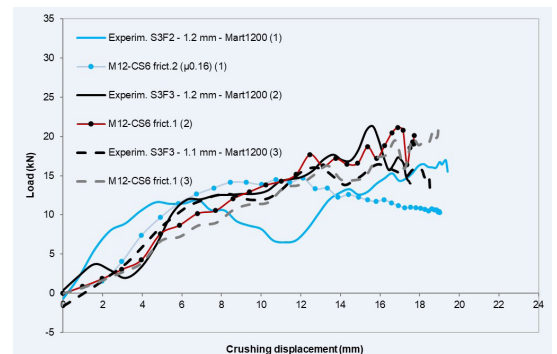


Figure 9. Comparison of load-crushing displacement histories of the experimental test for different prototypes and respective numerical models (index in parentheses is used to correspond the respective numerical model).

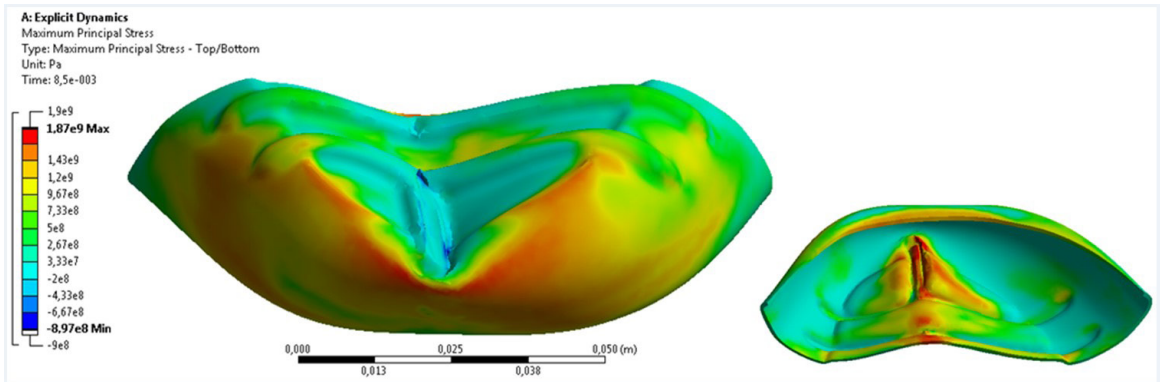


Figure 10. Numerical results for model S3F2 – 1.2mm – Mart1200. Principal stress gradient at the maximum impact test displacement time.

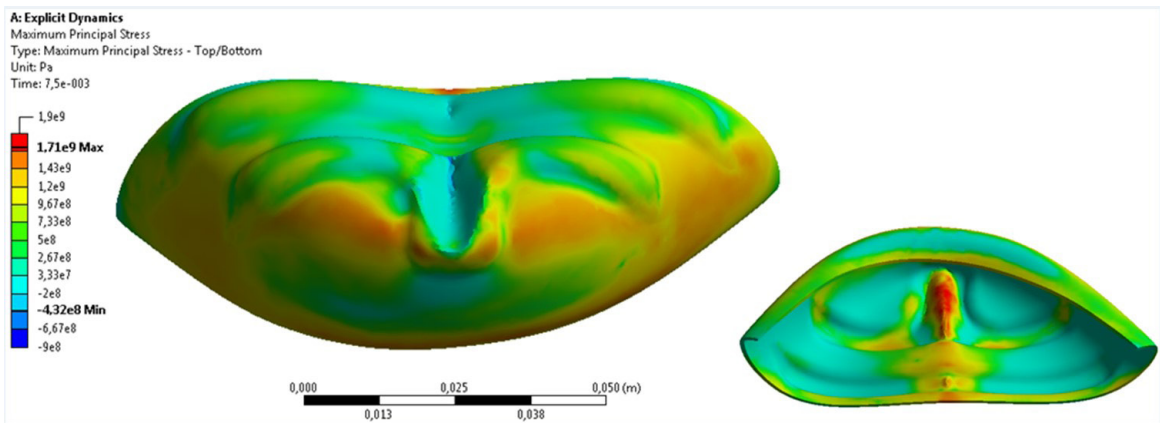


Figure 11. Numerical results for model S3F3 – 1.2mm – Mart1200. Principal stress gradient at the maximum impact test displacement time.

Table 3. Experimental and numerical results.

Toe Cap Model	$\delta$	$MfA$	$Pm$	$Pmax$	$E5$	$Ea(A)$	$Ea(A)/w$
Specimen	(mm)	(mm)	(kN)	(kN)	(J)	(J)	(J/kg)
S3F2 - 1.2 mm - Mart1200 (1)	19,42	(-)5,82	11,87	17,00	32,94	141,82	2170,76
M12-CS6 frict.2 ( $\mu 0.16$ ) (1)	19,00	(-)5,32	10,72	14,68	19,54	144,33	2109,36
S3F2 - 1.0 mm - Mart1200	23,32	(-)9,87	11,36 (7,11) <sup>(*)</sup>	37,33 (12,69)	25,03	109,77 (83,94)	2099,26 (1605,27)
S3F3 - 1.2 mm - Mart1200 (2)	17,54	(+)1,46	13,11	21,29	14,83	229,93	3504,96
M12-CS6 frict.1 (2)	17,72	(+)1,62	13,67	21,13	14,74	242,15	3332,35
S3F3 - 1.1 mm - Mart1200 (3)	18,50	(+)0,55	12,28	16,42	13,39	227,13	3840,51
M12-CS6 frict.1 (3)	18,93	(+)0,51	13,08	21,03	13,03	247,62	3717,53
S3F3 - 1.0 mm - Mart1200	23,03	(-)3,83	8,79	16,65	17,66	169,82	3113,76

$\delta$ : total crushing distance;  $MfA$ : Margin for Approval;  $P_{max}$ : peak load;  $E_5$ : energy absorbed in first 5 mm of crushing;  $E_a(A)$ : absorbed energy filtered only for the normative approval interval with positive performance; <sup>(\*)</sup> Values in parentheses in accordance with filtered corrections. <sup>(†)</sup> Numerical models are related to the experimental prototype respectively referenced.

material modelling with strain-rate dependence was able to reproduce the continuous load reaction promoted by the experimental evidence. The accuracy of the numerical model is here brought by the incorporation of a Cowper Symonds based- equation parameters, modelled with the UTS stress as reference within a range of 0.00025-100 s<sup>-1</sup>. Still, the non-linear behaviour revealed during the crash test conditions is challenging to describe in numerical simulations, coupled with changing conditions of friction and support. This can be associated with a non-predictable condition in

the normative testing for a thin toe cap wall in which the instability of response in the definition of the deformation model is higher. The focus on this topic can be taken in more depth in the reference<sup>21</sup>.

Furthermore, the challenge in the ongoing process of extreme thickness reduction demonstrates the exponential influence that it can have on the study variables. The ultimate thickness ratio at limit levels compromises the working role of other factors, in particular, the commitment of response possibly expected from any geometric model,

due to inevitable inertia problems. That accentuates crucial instability conditions in the behaviour mode, which tend to be difficult to heal. The 1.0 mm input variants, here added to the discussion, put emphasis on the structural challenging with severe conditions of impact deformation and thus they show their barriers with the overall results beyond the limit of any approval possibility, with severe damage, multi-local rupture, and the highest displacements in general. The experimental S3F2 1.0 mm prototype completely fails a satisfactory normative impact test regarding the maximum crushing distance, and it has collapsed and performed an uncontrolled deformation mode. However, at 6.8 ms of test time, a significant peak of load is raised which corresponds to a massive deceleration, as can be found graphically with the reduction of velocity at the end of test, and that can be related not only to the phenomenon of a collapse mode with critical folding events at the maximum deformation level, leading to a natural physic reaction of structural damping, but also, it is reasonable to accept that if the model has produced more local deformation and consequently a higher strain rate, it was able in these conditions to react and possibly to overcome a final recover.

Numerically, only an improved set of relief support conditions could have been considered, and even though presenting reliable quantitative results of crushing distance and approximating deformation shapes with similar compacting crash modes, they failed to predict the last peak of strength referred to this variant model. That raises other factors referred above, and once more, accentuates the counterbalance in comparison of experimental and numerical behaviours – The simulation does not predict the entire imprecision of the impact attack to the main geometric rib of the S3F2 model, locally or timely and, as consequence, they might not be under the same deformation rate conditions neither. Unlikely, and even for an equivalent extreme 1.0 mm variant, the S3F3 model was still able to promote a more stabilized and linear deform pattern, outcoming better numerical results qualitatively, and again, evolving key factors for final improvement in crashworthy performance.

## 5. Conclusions

In the present study, two following prototype models from the final development of a new light-weight slim metal toe cap for safety footwear were put in comparison. The improved S3F3 prototype made of an UHSS Mart1200 demonstrated capacity for an impact energy absorption up to a maximum ratio value of 3504,96 J/kg, 61% higher than the results achieved by the equivalent and precedent variant model S3F2. The research program performed the stabilization for a proof concept of an enhanced prototype from the ultimate S3F3 series, with 1.1 mm thickness in an order of 57 g mass, which it also leads to a performance in weight saving of around 65% comparatively to the benchmark toe cap model in steel alloy, and 17% compared to the composite/polymeric-based material, respectively.

Smaller crushing displacement, higher capacity to peak and mean load responses, and thus achieving greater values of energy absorption were able to perform by the S3F3 toe cap model with normative approval. Though, the limit borders about a feasible response to the crashworthiness

phenomenon were emerged in conditions of an extreme thickness optimization, challenging with mass reduction and local variable manufacturing effects. The expected loss of strength resulting from the thickness reduction was postponed to the limit with other potential parameters that countered into the ultimate results. The numerical modelling was able to predict them, fittingly in general, by the work hardening behaviour of the present case study, through sensitivity revealed when subjected to the impact conditions of a high strength material with its binomial outcome that was potentiated with structural geometric models worked on local stiffening. The improvement and understanding of a non-linear behaviour revealed during the crash test conditions raised up the greatest crashworthy performance.

## 6. Acknowledgments

The funding support from Projects I&DT Project S3 – Safety Slim Shoe, FCOMP-01-0202-FEDER-018458 is acknowledged.

## 7. References

1. Peixinho N, Costa S, Mendonça J. Impact behaviour of safety shoe high strength steel parts. *Engineering Transactions*. 2018;66(2):175-85.
2. European Union. European Parliament and of the Council. Regulation (EU) 2016/425 of the European Parliament and of the council of 9 March 2016 on personal protective equipment and repealing Council Directive 89/686/EEC. *Official Journal of the European Union*, EN, 2016; L81:51-98.
3. Janson D, Newman ST, Dhokia V. Next generation safety footwear. *Procedia Manufacturing*, 2019;38, 1668-1677.
4. Chong HC, Tennant LM, Kingston DC, Acker SM. Knee joint moments during high flexion movements: timing of peak moments and the effect of safety footwear. *Knee*. 2017;24(2):271-9.
5. Alkbir MFM, Sapuan SM, Nuraini AA, Ishak MR. Fibre properties and crashworthiness parameters of natural fibre-reinforced composite structure: a literature review. *Compos Struct*. 2016;148:59-73.
6. Kuhn M, Nowacki J, Himmel N. Development of an Innovative High Performance FRP Protective Toe Cap. *J Mater: Des Applications*. 2005;219(2):91-109.
7. Hsieh H, Hsieh M, Wang W. Safety toe cap made from nano composite material and preparation method of nano composite safety toe cap. *United States patent US 9,730,491*. 2017.
8. Fuhua L Composite material safety toe cap and manufacturing method thereof. *China patent CN103113733A*. 2014.
9. Janson D, Newman ST, Dhokia V. Safety footwear: a survey of end-users. *Appl Ergon*. 2021;92:103333.
10. Bianchi I, Forcellese A, Simoncini M, Vita A, Castorani V, Arganese M, et al. Life cycle impact assessment of safety shoes toe caps realized with reclaimed composite materials. *J Clean Prod*. 2022;347:131321.
11. Kropidłowska P, Irzmańska E, Zgórnjak P, Byczkowska P. Evaluation of the mechanical strength and protective properties of polycarbonate toe caps subjected to repeated impacts simulating workplace conditions. *Int J Occup Saf Ergon*. 2021;27:698-707.
12. Lee SM, Lim TS, Lee DG. Damage tolerance of composite toe cap. *Compos Struct*. 2005;67(2):167-74.
13. Nanda T, Singh V, Singh V, Chakraborty A, Sharma S. (2019). Third generation of advanced high-strength steels: processing routes and properties. *Proc Inst Mech Eng Pt L J Mater Des Appl*. 233(2), 209-238.

14. Tisza M. Development of lightweight steels for automotive applications. In: Sharma A, Duriagina Z, Kumar S, editors. *Engineering steels and high entropy-alloys*. London: IntechOpen; 2020.
15. Peixinho N, Pinho A. Study of viscoplasticity models for the impact behavior of high-strength steels. *J Comput Nonlinear Dyn*. 2007;2(2):114-23.
16. Peixinho N, Pinho A, Jones N. Determination of crash-relevant material properties for high-strength steels and constitutive equations. *SAE Trans*. 2002;1019-25.
17. Wang W, Li M, He C, Wei X, Wang D, Du H. Experimental study on high strain rate behavior of high strength 600–1000 MPa dual phase steels and 1200 MPa fully martensitic steels. *Mater Des*. 2013;47:510-21.
18. Costa SL, Mendonça JP, Peixinho N. Study on the impact behaviour of a new safety toe cap model made of ultra-high-strength steels. *Mater Des*. 2016;91:143-54.
19. CEN: European Committee for Standardization. EN ISO 22568-1:2019: foot and leg protectors – requirements and test methods for footwear components. Brussels, Belgium: CEN; 2019.
20. Peixinho N, Soares D, Vilarinho C, Pereira P, Dimas D. Experimental study of impact energy absorption in aluminium square tubes with thermal triggers. *Mater Res*. 2012;15(2):323-32.
21. Costa S. Development of advanced components for safety footwear - Integrated manufacturing methodology driven by impact events in mechanical design [thesis]. Braga, Portugal: Universidade do Minho; 2021.